JCAMECH

Vol. 51, No. 1, June 2020, pp 98-106
DOI: 10.22059/jcamech.2020.283714.414

Dynamic Response Determination of Viscoelastic Annular Plates Using FSDT – Perturbation Approach

Hamidreza Eipakchi[a] and Saeid Khadem Moshir[b]*

[a]*Faculty of Mechanical and Mechatronics Engineering, Shahrood University of Technology, Shahrood, I.R. IRAN*
[b]*Department of Mechanical, Industrial and Aerospace Engineering, Concordia University, Montreal, Quebec, Canada*

ARTICLE INFO

Article history:
Received: 17 June 2019
Accepted: 3 March 2020

Keywords:
Viscoelastic annular plate
Mathematical solution
Perturbation technique
Dynamic response
First order shear deformation theory

ABSTRACT

In this paper, the transient response of a viscoelastic annular plate which has time-dependent properties is determined mathematically under dynamic transverse load. The axisymmetric conditions are considered in the problem. The viscoelastic properties obey the standard linear solid model in shear and the bulk behavior in elastic. The equations of motion are extracted using Hamilton's principle by small deformation assumption for the elastic condition and they are extended to the viscoelastic form by defining viscoelastic operators based on separating the bulk and shear behaviors. The displacement field is defined with the first-order shear deformation theory by considering the transverse normal strain effect. These equations which contain four coupled partial differential equations *with* variable coefficients are solved using the perturbation technique. The results are compared with those obtained from the classical plate theory and the finite element method. The presented formulation is useful for parametric study because it does not need to generate a mesh and selecting time step for each model; Moreover, the running time is short concerning the finite element method. For sensitivity analysis, the effects of geometrical and mechanical parameters on the response are investigated by the parametric study.

1. Introduction

The viscoelastic materials are a class of advanced materials that have time-dependent properties. These materials can apply damping behavior in the structures. The damping is a significant dynamic parameter for investigating the vibrations, sound control, dynamic stability, positioning accuracy, fatigue endurance, and impact resistance. Moreover, many applications such as large space structures, engine blades, and high-speed machinery require the materials with light-weight and high dynamic performance which can be satisfied by viscoelastic materials. As a special case, an aircraft wheel and brake assembly have an axle with a circular flange which has contact with an *annular viscoelastic* plate [1]. In the medical science, the circular and annular viscoelastic plates are used as a contact lens-based in the bioactive agent delivery system which are systems for transferring of ophthalmic drugs and other bioactive agents to the eye [2]. It is shown that the response of polymer structures with the assumption of elastic behavior is inconsistent with reality. However, the viscoelastic theory is more suitable for describing their behavior [3]. Therefore, surveying the behavior of these structures is important in all aspects. In this paper, the *sensitivity* of the vibration response to input mechanical load and geometrical data is investigated. Robertson [4] investigated the forced axisymmetric motion of circular viscoelastic plates by applying the integer factorization algorithm and considering the rotary inertia and shear effects for a three-element viscoelastic model. Wang and Tsai [5] combined the Finite Elements (FE) and Newmark methods for quasi-static and dynamic analysis of viscoelastic Mindlin plates. They used the Maxwell and Standard Linear Solid (SLS) models for viscoelastic behavior. Chen [6] solved the quasi-static and dynamic responses of a linear viscoelastic beam using the FE method. Abdoun et al. [7] investigated the forced harmonic response of viscoelastic structures by an asymptotic numerical method. The FE method was used for the space discretization and the linear viscoelastic properties described by a complex relaxation matrix, which is a function of the load frequency. Assie et al. [8] presented a computational FE model for the impact response determination of viscoelastic frictionless bodies. The constitutive equations were expressed in the integral form. Khalfi and Ross [9] studied the transient response of a plate with partial constrained viscoelastic layer damping. They used the Prony series for viscoelastic core properties and Classical plate theory (CPT) assumption for formulation. They solved these equations using the fast Fourier transform method. Amoushahi and Azari [10] used a linear finite strip plate element based on the First-order Shear Deformation Theory (FSDT) for analyzing the viscoelastic plates. The mechanical properties were considered as a linear Prony series. Liang et al. [11] used the Differential Quadrature (DQ) and Laplace transform methods for three-dimensional transient analysis of Functionally Graded (FG) annular plates rests on a two-parameter viscoelastic foundation. The results were compared with the FE method. Gupta and Kumar [12] investigated the free

* Corresponding author. Email: web2-eipakchi@sharoodut.ac.ir

vibrations of a non-homogeneous viscoelastic circular plate with linearly varying thickness subjected to a linear temperature distribution based on the CPT and Kelvin constitutive model using Rayleigh-Ritz's method. Pawlus [13] presented the dynamic and buckling behavior of three-layered, annular plates with a liner viscoelastic core. The core was made of*polyurethane foam* which was modeled with the SLS constitutive model by considering CPT assumption. He used the orthogonality property for the circumferential variable, the finite difference for discretization in terms of the radial variable and Rung-Kutta's method to solve the obtained initial value problem. Furthermore, the problem was analyzed with the ABAQUS FE package. Panigrahi and Das [14] investigated the impact behavior of a sandwich plate with a filled polymeric foam core using the FE method. The impact load was due to a projectile penetration on the plate. Kumar and Panda [15] investigated the damping characteristics of a sandwich cylinder with a multilayered viscoelastic core by applying the FE simulation. Behera and Kumari [16] presented an exact solution for a composite rectangular plate using Zig-zag and third-order shear deformation theory. They used the Levy series and Kantorovich method for determining the natural frequencies. Arji et al. [17] [18] [19] [20] presented extensive studies on the nonlinear dynamic and vibration behaviors of viscoelastic nano-plates according to the CPT formulation. They defined the viscoelastic properties for Young's modulus with the Leaderman integral. The nano-plate had a rectangular shape with simply supported boundary conditions. Arji et al. [17] presented an analytical solution for nonlinear free and forced vibrations of viscoelastic nano-plates according to the couple stress theory. The solution was based on the double series method. Arji et al. [18] analyzed the primary and secondary resonances of viscoelastic nano-plates using the strain gradienttheory. The governing equations were solved using the harmonic balance and Runge-Kutta methods. Arji and Fakhrabadi [19] studied the nonlinear vibrations of viscoelastic nano-plates using modified couple stress theory. They used the Galerkin and Runge-Kutta methods for the solution. Arji et al. [20] investigated the nonlinear dynamic response of a bilayer rectangular biosensor with the strain gradient theory. The effects of viscoelasticity and flexoelectricity were considered as well. They used the multiple scale method for solution. Arji et al. [21] studied the nonlinear dynamics of a viscoelastic nano-plate using the modified couple stress theory. The coupled governing equations were solved with the Galerkin and Runge-Kutta methods.

To investigate the dynamic response of a structure theoretically, it is necessary to simulate it with a constitutive equation and then solve it. In most articles, the authors use the numerical method to solve the governing equation and finding the response of viscoelastic circular/annular plates. Those which use the analytical solution, usually apply the CPT for formulation. In this paper, we consider the following issues:

- The dynamic response of a viscoelastic annular plate which obeys the SLS model under dynamic distributed transverse load is presented based on the FSDT by considering transverse normal strain effect.
- The governing equations, which are a system of partial differential equations with variable coefficients, are solved analytically by using the perturbation technique.
- The FSDT results are compared with the FE and which has obtained from the CPT.
- A sensitivity analysis is performed and the effect of different parameters on the response is studied.

2. Governing equations

Consider an isotropic homogeneous annular plate with uniform thickness h, inner radius r_i, and outer radius r_o. The plate geometry is defined in a cylindrical coordinate system (r,θ,z). To extract the governing equations, the origin of the coordinate system is taken at the center of the mid-plane. The in-plane displacement components of an arbitrary point of the plate are U_r, U_θ, in the radial and circular directions and the out-of-plane component designated by U_z.

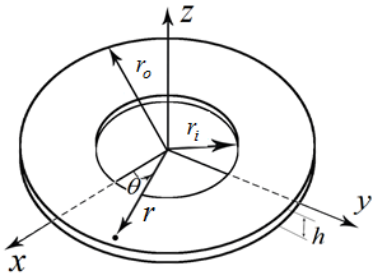

Figure 1. The geometry of a plate.

The displacement field is defined according to the FSDT assumption, in which the displacement components have linear variations in the z direction. For the axisymmetric case, we have

$$U_r(r,z,t) = u_0(r,t) + z.u_1(r,t); U_\theta(r,z,t) = 0$$
$$U_z(r,z,t) = w_0(r,t) + z.w_1(r,t) \quad (1)$$

Where u_0,w_0 denote the in-plane displacements of the mid-plane, z is the distance from the mid-plane and u_0,u_1,w_0,w_1 are unknown functions which depend on the radial coordinate r, and time parameter, t. The kinematic relations for small deflections are [22] :

$$\varepsilon_r = \frac{\partial U_r}{\partial r} = \frac{\partial u_0}{\partial r} + z\frac{\partial u_1}{\partial r}; \varepsilon_z = \frac{\partial U_z}{\partial z} = w_1$$
$$\varepsilon_\theta = \frac{U_r}{r} + \frac{1}{r}\frac{\partial U_\theta}{\partial \theta} = \frac{u_0 + zu_1}{r}; \gamma_{\theta z} = 0; \gamma_{r\theta} = 0 \quad (2)$$
$$\gamma_{rz} = \frac{\partial U_z}{\partial r} + \frac{\partial U_r}{\partial z} = \frac{\partial w_0}{\partial r} + u_1 + z\frac{\partial w_1}{\partial r}$$

The constitutive equations for an elastic structure can be written as follows [22]:

$$\sigma_r = (K - 2G/3)(\varepsilon_r + \varepsilon_\theta + \varepsilon_z) + 2G\varepsilon_r; \tau_{\theta z} = 0$$
$$\sigma_\theta = (K - 2G/3)(\varepsilon_r + \varepsilon_\theta + \varepsilon_z) + 2G\varepsilon_\theta; \tau_{r\theta} = 0 \quad (3)$$
$$\sigma_z = (K - 2G/3)(\varepsilon_r + \varepsilon_\theta + \varepsilon_z) + 2G\varepsilon_z; \tau_{rz} = G\gamma_{rz}$$

Where G and K are the shear and bulk moduli, respectively. The kinetic energy T and the strain energy U are expressed as the following:

$$T = \frac{1}{2}\int_0^{2\pi}\int_{r_i}^{r_o}\int_{-h/2}^{h/2} \rho\left(\dot{U}_r^2 + \dot{U}_\theta^2 + \dot{U}_z^2\right) r\, dr d\theta dz \quad (4a)$$

$$U = \frac{1}{2}\int_0^{2\pi}\int_{r_i}^{r_o}\int_{-h/2}^{h/2} \left(\sigma_r\varepsilon_r + \sigma_\theta\varepsilon_\theta + \sigma_z\varepsilon_z + \tau_{rz}\gamma_{rz}\right) r\, dr d\theta dz \quad (4b)$$

Where $\rho$is the plate density. The external work due to lateral distributed stress, which is applied to the plate surface ($z=h/2$) is as follows:

$$W_Q = \int_0^{2\pi}\int_{r_i}^{r_o} Q(r,t)U_z(r,z,t)\big|_{z=h/2}\, r\, dr d\theta \quad (4c)$$

$Q(r,t)$ is positive upward. By applying Hamilton's principle, the equations of motion and the boundary conditions can be determined as:

$$\delta\int_{t_1}^{t_2} L dt = 0;\ L = T - U - W_Q \tag{4d}$$

From Eqs. (4), four equations are derived in terms of stress resultants for the elastic plate as the following.

$$\begin{aligned}
&\frac{\partial}{\partial r}(r\,\mathrm{N}_r) - N_\theta - \rho r h\frac{\partial^2 u_0}{\partial t^2} = 0\\
&\frac{\partial}{\partial r}(r\,\mathrm{M}_r) - \mathrm{M}_\theta - r Q_r - \frac{\rho r h^3}{12}\frac{\partial^2 u_1}{\partial t^2} = 0\\
&\frac{\partial}{\partial r}(r Q_r) - \rho r h\frac{\partial^2 w_0}{\partial t^2} - r Q(r,t) = 0\\
&\frac{1}{r}\frac{\partial}{\partial r}(r M_{rz}) - N_z - \frac{\rho h^3}{12}\frac{\partial^2 w_1}{\partial t^2} - \frac{1}{2}hQ(r,t) = 0
\end{aligned} \tag{5a}$$

The boundary conditions are:

$$\left(r(N_r\delta u_0 + M_r\delta u_1 + Q_r\delta w_0 + M_{rz}\delta w_1)\right)\Big|_{r_i}^{r_o} = 0 \tag{5b}$$

Where the stress resultants are defined as follows:

$$\begin{aligned}
&\left(N_r, N_\theta, N_z\right) = \int_{-h/2}^{h/2}(\sigma_r, \sigma_\theta, \sigma_z)\,dz\\
&\left(M_r, M_\theta\right) = \int_{-h/2}^{h/2} z\left(\sigma_r, \sigma_\theta\right)dz\\
&(Q_r, M_{rz}) = K_S\int_{-h/2}^{-h/2}(1, z)\tau_{rz}\,dz
\end{aligned} \tag{5c}$$

K_s is the shear correction factor which is assumed as $\pi^2/12$ [23].By substituting Eqs. (5c) into Eqs. (5a), the equations of motion are extracted for the *elastic* plate in terms of displacement components as follows.

$$a_6\cdot\left(\frac{\partial}{\partial r}(r\frac{\partial u_0}{\partial r}) - \frac{u_0}{r}\right) + (K - \frac{2}{3}G)r\frac{\partial w_1}{\partial r} - \rho r\frac{\partial^2 u_0}{\partial t^2} = 0 \tag{6a}$$

$$a_6\cdot\frac{h^2}{12}\left(\frac{\partial}{\partial r}(r\frac{\partial u_1}{\partial r}) - \frac{u_1}{r}\right) - K_S G r(u_1 + \frac{\partial w_0}{\partial r}) - \frac{\rho r h^2}{12}\frac{\partial^2 u_1}{\partial t^2} = 0 \tag{6b}$$

$$K_S G h\frac{\partial}{\partial r}\left(r(\frac{\partial w_0}{\partial r} + u_1)\right) - \rho r h\frac{\partial^2 w_0}{\partial t^2} - r Q(r,t) = 0 \tag{6c}$$

$$\begin{aligned}
&K_S G\frac{h^2}{12}\frac{\partial}{\partial r}(r\frac{\partial w_1}{\partial r}) - (K - \frac{2}{3}G)\frac{\partial}{\partial r}(ru_0) - a_6 r w_1\\
&-\frac{\rho r h^2}{12}\frac{\partial^2 w_1}{\partial t^2} - \frac{1}{2}r Q(r,t) = 0; a_6 = K + \frac{4}{3}G
\end{aligned} \tag{6d}$$

In the viscoelastic analysis, it is usual to separate the deviatoric and dilatational parts of the stress components. For the deviatoric part $P_1\tau_{ij}=Q_1\gamma_{ij}$, and for dilatation, $P_2\sigma_{ii}=Q_2\varepsilon_{ii}$. Where P_1, Q_1, P_2, Q_2 are viscoelastic operators, τ_{ij}, γ_{ij} denote the shear stress and strain, respectively and σ_{ii}, ε_{ii} are the traces of the stress and strain tensors. In the elastic case, the shear stress-strain relation is $\tau_{ij}=2G\varepsilon_{ij}$, so $G=Q_1/2P_1$ and the bulk modulus is $K=Q_2/3P_2$. We assume that the *viscoelastic property obeys the SLS model in shear* and *elastic in bulk* i.e. $K=K_0$ where K_0 is a constant (elastic bulk modulus). We consider an SLS model with spring elements G_1, G_2, and damping element η as Fig. 2. The behavior of this model in the relaxation and creep has adaptation with the reality and it can convert to the Kelvin, Maxwell or elastic elements in special cases as follows:

a) If $\eta\to\infty$; an elastic element with equivalent shear modulus G_e is obtained where $1/G_e=1/G_1+1/G_2$.
b) If $\eta\to 0$; an elastic element with equivalent shear modulus $G_e = G_1$ is obtained.
c) If $G_2\to 0$; a Maxwell element is achieved.
d) If $G_1\to\infty$; a Kelvin element is yielded.

The viscoelastic operators for *SLS* model can express as [24]:

$$P_1 = (\frac{1}{G_1} + \frac{1}{G_2}) + \frac{\tau}{G_1}D;\ P_2 = 1;\ Q_1 = 2(1+\tau D);\ Q_2 = 3K_0 \tag{7}$$

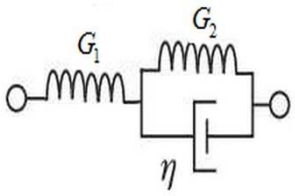

Figure 2. Standard linear solid model (SLS).

Where $\tau=\eta/G_2$ is the relaxation time and $D=\partial/\partial t$ is the time derivative operator. By substituting G in terms of viscoelastic operators into Eqs. (6) and applying the time derivative operator on the equations, the governing equations of motion for viscoelastic material are derived as the general following form:

$$\begin{aligned}
&L_1[u_0, w_1, r, t, \partial/\partial t, \partial^2/\partial t^2, \partial^3/\partial t^3,\\
&\quad \partial/\partial r, \partial^2/\partial r^2, \partial^3/\partial r^2\partial t, \partial^2/\partial r\partial t] = 0
\end{aligned} \tag{8a}$$

$$\begin{aligned}
&L_2[u_1, w_0, w_1, r, t, \partial/\partial t, \partial^2/\partial t^2, \partial^3/\partial t^3,\\
&\quad \partial/\partial r, \partial^2/\partial r^2, \partial^3/\partial r^2\partial t, \partial^2/\partial r\partial t] = 0
\end{aligned} \tag{8b}$$

$$\begin{aligned}
&L_3[u_1, w_0, w_1, r, t, Q, \partial/\partial t, \partial^2/\partial t^2, \partial^3/\partial t^3,\\
&\quad \partial/\partial r, \partial^2/\partial r^2, \partial^3/\partial r^2\partial t, \partial^2/\partial r\partial t] = 0
\end{aligned} \tag{8c}$$

$$\begin{aligned}
&L_4[u_0, w_1, r, t, Q, \partial/\partial t, \partial^2/\partial t^2, \partial^3/\partial t^3,\\
&\quad \partial/\partial r, \partial^2/\partial r^2, \partial^3/\partial r^2\partial t, \partial^2/\partial r\partial t] = 0
\end{aligned} \tag{8d}$$

Where L_1 to L_4 are differential operators. The explicit dimensionless forms of these equations will be reported later. Eqs. (8) contain four coupled partial differential equations with variable coefficients. There are different numerical and analytical methods for the solution of the equations with variable coefficients including:

- The Frobenius series method is the popular method and it was used widely in 1980-1990 especially for analysis of structures with variable thicknesses e.g. Suzuki et al. [25]. This method has long calculations and its convergence may be slow.
- The numerical methods including DQ, and FE methods.
- The ring method which converts the plate to some narrow rings and solves the equations for each ring analytically and finally applies the continuity conditions between the rings. Note that for each ring, we have the equations with constant coefficients. The appropriated number of rings is important for convergence. This solution procedure is cumbersome.
- The Ritz method.
- Converting the governing equations to equations with constant coefficients with appropriate transformation. This method may be used for the problems with one governing equations (CPT) such as the Euler-Bernoulli equation. In this paper, the perturbation technique in conjunction with a new transformation is used to solve the equations. This method can convert the governing equations to equations with constant coefficients in each order. Besides, the coupling of equations can be reduced and one can obtain two systems of equations, each system is coupled which has constant coefficients.

3. Analytical solution

The *perturbation* technique is used for the analytical solution. Before using this method, it is necessary to convert the equations to the dimensionless form. One can define the following dimensionless quantities.

$$r^*=\frac{r}{a};\ h^*=\frac{h}{h_0};\ t^*=\frac{t}{t_0};\ u_0^*(r^*,t^*)=\frac{u_0(r,t)}{h_0};$$
$$u_1^*(r^*,t^*)=u_1(r,t);\ w_0^*(r^*,t^*)=\frac{w_0(r,t)}{h_0};\qquad (9a)$$
$$w_1^*(r^*,t^*)=w_1(r,t);\ Q^*(r^*,t^*)=\frac{Q(r,t)}{K_0}$$

One can substitute Eqs. (9a) into governing equations (8).The following dimensionless parameters can be expressed.

$$\varepsilon=\frac{h_0}{a};\ e=(\frac{h_0}{ct_0})^2;\ \beta=\frac{\tau}{t_0};\ G_0^*=K_0(\frac{1}{G_1}+\frac{1}{G_2});$$
$$G_1^*=\frac{K_0}{G_1};\ c=\sqrt{K_0/\rho}\qquad (9b)$$

where $r^*$and t^* are dimensionless location and time, respectively.u_0^*,u_1^*,w_0^*,w_1^* are dimensionless displacement components. a, h_0 and t_0 are the characteristic radius, thickness and time, respectively, which are defined as $a=r_o$, $h_0=h$,and$t_0=a/c$. c is a quantity with the speed dimension. ε is a small parameter that is considered as the *perturbation parameter*. By using Eqs. (9) and defining the transformation $\boldsymbol{X=(r^*-1)/\varepsilon}$, the dimensionless form of the governing equations (in terms of displacement) can be derived. The method of multiple scales is used for the solution. The new scale $T_0=t^*$, $T_1=\varepsilon t^*$ are defined. We have [26]:

$$\frac{\partial}{\partial t^*}=\frac{\partial}{\partial T_0}+\varepsilon\frac{\partial}{\partial T_1};\ \frac{\partial^2}{\partial t^{*2}}=\frac{\partial^2}{\partial T_0^2}+2\varepsilon\frac{\partial^2}{\partial T_0\partial T_1};$$
$$\frac{\partial^3}{\partial t^{*3}}=\frac{\partial^3}{\partial T_0^3}+3\varepsilon\frac{\partial^3}{\partial T_0^2\partial T_1}\qquad (10)$$

Substituting Eqs. (9 and 10) into Eqs. (8), the dimensionless forms of the governing equations (in terms of displacement components) are derived as follows.

$$eq_1:\ 6L_{11}[u_0^*,w_1^*]+6\varepsilon(2L_{11}[u_0^*,w_1^*].X+A_{12})$$
$$+\varepsilon^2 f_{11}(u_0^*,w_1^*,\varepsilon)=0;\ L_{11}[u_0^*,w_1^*]=g_{32}[u_0^*,a_0,a_1]$$
$$+g_{33}[w_1^*,b_0,b_1]-eg_{51}[u_0^*];A_{12}=\frac{\partial}{\partial X}g_{35}[u_0^*,\beta a_1,a_0]\qquad (11a)$$
$$-2e\frac{\partial^2}{\partial T_0\partial T_1}g_{35}[u_0^*,\frac{3}{2}\beta G_1^*,G_0^*]+\beta\frac{\partial^2}{\partial X\partial T_1}(a_1\frac{\partial u_0^*}{\partial X}+b_1w_1^*)$$

$$eq_2:\ 3L_{12}[u_1^*,w_0^*]+3\varepsilon(2L_{12}[u_1^*,w_0^*].X+A_{22})$$
$$+\varepsilon^2 f_{12}(u_1^*,w_0^*,\varepsilon)=0;$$
$$L_{12}[u_1^*,w_0^*]=h^{*2}(g_{32}[u_1^*,a_0,a_1]-e\,g_{51}[u_1^*])$$
$$-12K_s(\frac{\partial}{\partial X}g_{35}[w_0^*,\beta,1]+g_{35}[u_1^*,\beta,1])$$

$$A_{22}=-3eh^{*2}\frac{\partial^2}{\partial T_0\partial T_1}g_{35}[u_1^*,\beta G_1^*,\frac{2}{3}G_0^*]\qquad (11b)$$
$$+\beta h^{*2}a_1\frac{\partial}{\partial X}(\frac{\partial^2u_1^*}{\partial X\partial T_1}+\frac{\partial u_1^*}{\partial T_0})+h^{*2}a_0\frac{\partial u_1^*}{\partial X}$$
$$-12K_s\beta\frac{\partial}{\partial T_1}(\frac{\partial w_0^*}{\partial X}+u_1^*)$$

$$eq_3:L_{13}[u_1^*,w_0^*]-g_{35}[Q^*,\beta G_1^*,G_0]+\varepsilon((L_{13}[u_1^*,w_0^*]$$
$$-g_{35}[Q^*,\beta G_1^*,G_0])X+A_{32})+\varepsilon^2 f_{13}(u_1^*,w_0^*,\varepsilon)=0;$$
$$L_{13}[u_1^*,w_0^*]=h^*(K_sg_{32}[w_0^*,1,1]-eg_{51}[w_0^*]$$
$$+K_s\frac{\partial}{\partial X}g_{35}[u_1^*,\beta,1]);\ A_{32}=h^*(K_s(g_{35}[u_1^*,\beta,1]\qquad (11c)$$
$$+\frac{\partial g_{35}[w_0^*,\beta,1]}{\partial X}+\beta\frac{\partial^2}{\partial X\partial T_1}(\frac{\partial w_0^*}{\partial X}+u_1^*))$$
$$-2e\frac{\partial^2}{\partial T_0\partial T_1}g_{35}[w_0^*,\frac{3}{2}\beta G_1^*,G_0^*])$$

$$eq_4:L_{14}[u_0^*,w_1^*]-6g_{35}[Q^*,\beta G_1^*,G_0]+\varepsilon((L_{14}[u_0^*,w_1^*]$$
$$-6g_{35}[Q^*,\beta G_1^*,G_0]).X+A_{42})+\varepsilon^2 f_{14}(u_0^*,w_1^*,\varepsilon)=0;$$
$$L_{14}[u_0^*,w_1^*]=h^{*2}(K_sg_{32}[w_1^*,1,1]-eg_{51}[w_1^*])$$
$$-12(\frac{\partial}{\partial X}g_{35}[u_0^*,\beta b_1,b_0]-2g_{35}[w_1^*,\beta a_1,a_0])$$
$$A_{42}=K_sh^{*2}g_{33}[w_1^*,1,1]-2eh^{*2}\frac{\partial^2}{\partial T_0\partial T_1}\qquad (11d)$$
$$g_{35}[w_1^*,\frac{3}{2}\beta G_1^*,G_0^*]-12g_{35}[u_0^*,\beta b_1,b_0]$$
$$+K_s\beta h^{*2}\frac{\partial^3w_1^*}{\partial X^2\partial T_1}-12\beta\frac{\partial}{\partial T_1}(b_1\frac{\partial u_0^*}{\partial X}+a_1w_1^*)$$

Where:

$$g_{35}[y,a,b]=a\frac{\partial y}{\partial T_0}+b.y;a_0=G_0^*+\frac{4}{3};\ a_1=G_1^*+\frac{4}{3};$$
$$g_{33}[y,a,b]=a\frac{\partial y}{\partial X}+\beta b\frac{\partial^2y}{\partial X\partial T_0}=\frac{\partial}{\partial X}g_{35}[y,\beta b,a];$$
$$g_{32}[y,a,b]=\frac{\partial}{\partial X}g_{33}[y,a,b]=\frac{\partial^2}{\partial X^2}g_{35}[y,\beta b,a];\qquad (11e)$$
$$g_{51}[y]=\beta G_1^*\frac{\partial^3y}{\partial T_0^3}+G_0^*\frac{\partial^2y}{\partial T_0^2}=\frac{\partial^2}{\partial T_0^2}$$
$$g_{35}[y,\beta G_1^*,G_0^*];\ b_0=G_0^*-\frac{2}{3};\ b_1=G_1^*-\frac{2}{3};$$
$$u_0^*=u_0^*(X,T_0,T_1);u_1^*=u_1^*(X,T_0,T_1);$$
$$w_0^*=w_0^*(X,T_0,T_1);\ w_1^*=w_1^*(X,T_0,T_1)$$

$f_{11},f_{12},f_{13},f_{14}$ are functions of dependent variables which do not appear in our selected expansions (Eqs. 12).We seek a straightforward expansion for the solution as follows.

$$u_0^*(X,T_0,T_1;\varepsilon)=u_{00}^*(X,T_0,T_1)+\varepsilon u_{01}^*(X,T_0,T_1);$$
$$u_1^*(X,T_0,T_1;\varepsilon)=u_{10}^*(X,T_0,T_1)+\varepsilon u_{11}^*(X,T_0,T_1);$$
$$w_0^*(X,T_0,T_1;\varepsilon)=w_{00}^*(X,T_0,T_1)+\varepsilon w_{01}^*(X,T_0,T_1);\qquad (12)$$
$$w_1^*(X,T_0,T_1;\varepsilon)=w_{10}^*(X,T_0,T_1)+\varepsilon w_{11}^*(X,T_0,T_1)$$

One can substitute Eqs. (12) into Eqs. (11) and equate the terms with the same power of ε to zero. The governing equations with order-zero can be extracted as follows.

$$eq_1:L_{11}[u_{00}^*,w_{10}^*]=0;$$
$$eq_4:L_{14}[u_{00}^*,w_{10}^*]-6g_{35}[Q^*,\beta G_1^*,G_0]=0\qquad (13a)$$

$$eq_2:L_{12}[u_{10}^*,w_{00}^*]=0;$$
$$eq_3:L_{13}[u_{10}^*,w_{00}^*]-g_{35}[Q^*,\beta G_1^*,G_0]=0\qquad (13b)$$

Note that Eqs. (6 and 8) are *four coupled partial differential equations with variable coefficients*. By defining the parameter X, one can convert the governing equations with *variable coefficients* to a system of equations with *constant equations* in each order of ε. Eqs. (13a and13b) can be solved separately, or there are two non-homogenous systems of coupled partial differential equations. The governing equations with order-one are as the following.

$$eq_1:L_{11}[u_{01}^*,w_{11}^*]=FF_1;eq_4:L_{14}[u_{01}^*,w_{11}^*]=FF_4;$$
$$FF_1=-2L_{11}[u_{00}^*,w_{10}^*].X-A_{12}[u_{00}^*,w_{10}^*];$$
$$FF_4=-(L_{14}[u_{00}^*,w_{10}^*]-6g_{35}[Q^*,\beta G_1^*,G_0]).X\qquad (14a)$$
$$-A_{42}[u_{00}^*,w_{10}^*]$$

$$eq_2:L_{12}[u_{11}^*,w_{01}^*]=FF_2;\ eq_3:L_{13}[u_{11}^*,w_{01}^*]=FF_3;$$
$$FF_2=-2L_{12}[u_{10}^*,w_{00}^*].X-A_{22}[u_{10}^*,w_{00}^*];$$
$$FF_3=-(L_{13}[u_{10}^*,w_{00}^*]-g_{35}[Q^*,\beta G_1^*,G_0]).X\qquad (14b)$$
$$+A_{32}[u_{10}^*,w_{00}^*]$$

The solution of the second system (Eqs. 13b) according to the eigenfunction expansion method is set as the following:

$$u_{10}^{*}(X,T_0,T_1)=\sum_{m=1}^{\infty}A_{1m}(T_0,T_1)\phi_{2m}(\mathrm{X});\quad w_{00}^{*}(X,T_0,T_1)=\sum_{m=1}^{\infty}A_{2m}(T_0,T_1)\phi_{3m}(\mathrm{X}) \tag{15a}$$

Where φ_{2m}, φ_{3m} are the solutions of the homogenous parts of Eqs. (13b) (mode shapes). Khadem et al. [27] explained the procedure of finding the mode shapes for different boundary conditions. For a *simply supported* annular plate, the mode shapes can be considered as follows.

$$\phi_{2m}=\cos(\alpha_{\mathrm{m}}\mathrm{X});\ \phi_{3m}=\sin(\alpha_{\mathrm{m}}\mathrm{X});\alpha_{\mathrm{m}}=\frac{m\pi}{L};\quad L=X_{out}-X_{in};X_{out}=X\big|_{r=r_o};X_{in}=X\big|_{r=r_i} \tag{15b}$$

The formulations for the general boundary conditions are explained in Appendix A. For simply supported boundary conditions, we substitute Eqs. (15a and b) into Eqs. (13b). It is yielded:

$$\sum_{m=1}^{\infty}P_{1m}\cos(\alpha_{\mathrm{m}}\mathrm{X})=0\ ;\ \sum_{m=1}^{\infty}P_{2m}\sin(\alpha_{\mathrm{m}}\mathrm{X})=F_2 \tag{15c}$$

Where:

$$\begin{aligned}&g_{32}[w_{00}^{*},a,b]=-\alpha_m{}^2 g_{35}[A_{2m},\beta b,a];\\&g_{32}[u_{10}^{*},a,b]=-\alpha_m{}^2 g_{35}[A_{1m},\beta b,a];\\&P_{1m}=-h^{*2}\left(\alpha_m{}^2 g_{35}[A_{1m},\beta a_1,a_0]+eg_{51}[A_{1m}]\right)\\&-12K_S(\alpha_m g_{35}[A_{2m},\beta,1]+g_{35}[A_{1m},\beta,1])\\&P_{2m}=-h^{*}(K_S\alpha_m{}^2 g_{35}[A_{2m},\beta,1]+eg_{51}[A_{2m}])\\&-K_S\alpha_m g_{35}[A_{1m},\beta,1]);F_2=g_{35}[Q^{*},\beta G_1^{*},G_0]\end{aligned} \tag{15d}$$

F_2 is the non-homogenous part of the second equation which is a function of Q^{*}. P_{1m} and $P_{2m}$are expressions in terms of $A_{1m}(T_0,T_1)$and $A_{2m}(T_0,T_1)$.$P_{1m}$and $P_{2m}$are obtained from the Fourier half-range expansion formula as the following:

$$P_{1m}=\frac{2}{L}\int_{X_{in}}^{X_{out}}F_1\cos(\alpha_m X)dX;\quad P_{2m}=\frac{2}{L}\int_{X_{in}}^{X_{out}}F_2\sin(\alpha_m X)dX \tag{15e}$$

Eqs. (15e) are two coupled ordinary differential equations which their homogenous solutions are in the following form:

$$A_{1m}(T_0,T_1)=\sum_{j=1}^{6}a_j(T_1)e^{i\alpha_j T_0};\quad A_{2m}(T_0,T_1)=\sum_{j=1}^{6}b_j(T_1)e^{i\alpha_j T_0} \tag{15f}$$

Where α_j(j=1..6) are the eigenvalues of Eqs. (15f). By substituting Eqs. (15f) into homogenous part of Eqs. (15e), two homogenous algebraic equations can be found. α_j's are the eigenvalues and $a_j(T_1)$, $b_j(T_1)$are its eigenvector elements. The particular solutions of Eqs. (15e) depend on the non-homogenous part of equations. The solution procedure of Eqs. (13a) is the same as the mentioned method. In solving equations order-one e.g. Eqs. (14b), the solution for the simply supported case is considered as the following.

$$u_{11}^{*}(X,T_0,T_1)=\sum_{m=1}^{\infty}A_{3m}(T_0,T_1)\cos(\alpha_{\mathrm{m}}\mathrm{X});\quad w_{01}^{*}(X,T_0,T_1)=\sum_{m=1}^{\infty}A_{4m}(T_0,T_1)\sin(\alpha_{\mathrm{m}}\mathrm{X}) \tag{16a}$$

By substituting Eqs. (16a, 15a) into Eqs.(14b), we have:

$$\sum_{m=1}^{\infty}P_{3m}\cos(\alpha_{\mathrm{m}}\mathrm{X})=FF_2\ ;\ \sum_{m=1}^{\infty}P_{4m}\sin(\alpha_{\mathrm{m}}\mathrm{X})=FF_3 \tag{16b}$$

Where:

$$P_{3m}=\frac{2}{L}\int_{X_{in}}^{X_{out}}FF_2\cos(\alpha_m X)dX;\quad P_{4m}=\frac{2}{L}\int_{X_{in}}^{X_{out}}FF_3\sin(\alpha_m X)dX \tag{16c}$$

FF_2 and FF_3 are expressions in terms of $exp(i\alpha_jT_0)$,$sin(\alpha_mX)$ and $cos(\alpha_mX)$ and P_{3m} and P_{4m} are in terms of $A_{3m}(T_0,T_1)$ and $A_{4m}(T_0,T_1)$.The non-homogenous part of Eqs. (16c) which includes $exp(i\alpha_jT_0)$,(j=1..6) are secular terms. Before solving Eqs. (16c), it is necessary to remove the secular terms. To this purpose, we use the solvability condition [26]. The secular terms of the particular solutions of Eqs. (16c) are considered as the following.

$$A_{3m}(T_0,T_1)=\sum_{j=1}^{6}d_j\left(T_1\right)\exp(i\alpha_j T_0);\quad A_{4m}(T_0,T_1)=\sum_{j=1}^{6}g_j\left(T_1\right)\exp(i\alpha_j T_0) \tag{17}$$

By substituting Eqs. (17) into Eqs. (16c) and setting the terms with coefficients $exp(i\alpha_jT_0)$ (j=1..6) to zero, we find a system of first-order ordinary differential equations for determining $a_j(T_1)$. The constants of the solution are calculated by considering the zero initial conditions.

4. Classical plate theory

For CPT, the equation of motion for the elastic circular/annular plate in the polar coordinate system can be written as [28]:

$$D_0\nabla^4 w_0+\rho h\frac{\partial^2 w_0}{\partial t^2}=Q(r,t);\quad \nabla^2=\frac{1}{r}\frac{\partial}{\partial r}(r\frac{\partial}{\partial r});D_0=\frac{Eh^3}{12(1-\nu^2)} \tag{18a}$$

Moreover, we have:

$$E=\frac{9KG}{3K+G};\ \nu=\frac{3K-2G}{6K+2G} \tag{18b}$$

By substituting $G=Q_1/2P_1$ and $K=K_0$ into Eqs. (18b), the flexural rigidity D_0 is obtained for the viscoelastic plate. For a plate which is viscoelastic in shear and elastic in bulk and using Eq. (7) for the SLS model, the governing equation for a viscoelastic plate according to CPT is determined. By using Eqs. (18), the governing equation is converted to a dimensionless equation as the following:

$$\begin{aligned}&eq: L_{15}[w_0^{*}]+A_{62}[Q^{*},d_{12},d_{11},d_{10}]\\&+\varepsilon((3L_{15}[w_0^{*}]+A_{62}[Q^{*},d_{22},d_{21},d_{20}]).X+A_{52})\\&+\varepsilon^2 f_{15}(w_0^{*},Q^{*},\varepsilon)=0;\\&L_{15}[w_0^{*}]=\frac{\partial^4}{\partial X^4}A_{62}[w_0^{*},d_6,d_5,d_4]\\&+\frac{\partial^2}{\partial T_0{}^2}A_{62}[w_0^{*},d_{40},d_3,d_2];\\&A_{52}=\frac{\partial^2}{\partial T_1\partial T_0}A_{62}[w_0^{*},4d_{40},3d_3,2d_2]\\&+\frac{\partial^4}{\partial X^4}g_{35}[w_0^{*},2d_6,d_5]+\frac{2\partial^3}{\partial X^3}A_{62}[w_0^{*},d_6,d_5,d_4];\\&A_{62}[y,p_2,p_1,p_0]=p_2\frac{\partial^2 y}{\partial T_0{}^2}+p_1\frac{\partial y}{\partial T_0}+p_0 y\end{aligned} \tag{19a}$$

Where:

$$d_6 = 3G_1^*\beta^2 h^{*3} a_3;\ d_5 = 3G_1^*\beta h^{*3}(a_2 + a_3);\ a_2 = G_0^* + \frac{1}{3};$$
$$d_4 = 3G_1^* h^{*3} a_2;\ d_2 = 9eG_0^* G_1^* h^* a_0;\ d_{22} = -27G_1^*\beta^2 a_1;$$
$$d_{40} = 9eG_1^{*2}\beta^2 h^* a_1;\ d_3 = 9eG_1^*\beta h^*(G_1^* a_0 + G_0^* a_1); \quad (19b)$$
$$d_{11} = 18\beta(b_1 G_0^* - 2a_2 G_1^*);\ d_{12} = -9G_1^*\beta^2 a_1;\ a_3 = G_1^* + \frac{1}{3};$$
$$d_{20} = -27G_0^* a_0;\ d_{21} = 54\beta(b_0 G_1^* - 2a_3 G_0^*);\ d_{10} = -9G_0^* a_0$$

By applying the perturbation technique as explained before, the response can be determined.

5. Numerical analysis

Ansys12 FE package has been used for the numerical analysis. The selected elements are PLANE 182 and SOLID 186 that have viscoelastic feature-capability [29]. The boundary conditions are assumed simply supported at both edges. To achieve convergence, the number of elements and the time step were selected by trial and error. We used the frequency analysis for different mesh sizes and time history response of the middle radius for time step selection. The time step was chosen 0.002s. The geometrical and material properties of the plate have been listed in Table 1. The selected material is a kind of silicone polymer which is used for contact lens-based bioactive agent delivery system and its viscoelastic properties in shear (G_1, G_2,η) has been reported by [2]. The transverse load is a pulse load and it acts for 1 second as the $Q(r,t)=q_0(1-H(t-1))$ where q_0=5 N/m^2 and $H(t)$ stands for the Heaviside step function.

Table 1. Geometrical and material properties

Outer radius (m)	r_o=0.15
Inner radius (m)	r_i=4.5e-2
Thickness (m)	h=7.5e-3
Poisson's ratio	ν=0.25
Viscoelastic modulus (Pa)	G_1=5.5e5, G_2=9e5
Viscosity coefficient (Pa.s)	η=7.6e4
Bulk module (Pa)	K_0=9.16e5
Density (kg/m^3)	ρ=1500

6. Results

The presented formulation is used to program in the mathematical environment Maple 15. By using this formulation, one can find the response easily and fast for different load profiles. It is noted that in the presented graphs, $Uz^*= Uz/h_0$.

6.1. Comparison of results

The FSDT, CPT, and FE results for the transverse response of the middle surface at mid-radius $r=(r_i+r_o)/2$ and a point near the outer edge (r^*=0.933) have been shown in Figs. 3, 4. The CPT has a time delay in response with respect to the FSDT and FE. The FSDT response is closer to the FE than the CPT (except that at the start of loading) and the oscillation frequency of the FSDT is in a good agreement with the FE with respect to the CPT. The obtained amplitude of displacement using the FSDT is smaller than FE and CPT results. Moreover, the difference between CPT and both the FE and FSDT increases near the boundary.

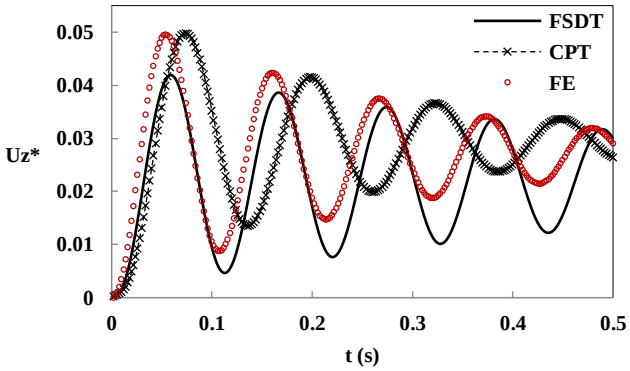

Figure 3. Transverse response at mid-radius $r=(r_i+r_o)/2$.

One of the advantages of the FSDT is its ability to calculate the radial response. Fig. 5 shows the radial response of the plate at r^*=0.767 and $z=h/2$ by the FSDT and FE. The radial deflection of the FSDT is smaller than the FE.

6.2. Sensitivity analysis

The effect of modulus G_1 on the transverse response has been shown in Fig. 6. Increasing G_1 decreases the average deflection and increases the oscillation frequency which is due to an increase in the stiffness of the plate.

6.3. Load profile

The presented results were related to a pulse load with constant amplitude. By changing the load profile, the particular solution of Eqs. (13 and14) will be affected. For instance, one can calculate the results for a load as $Q(X,t)=q_0Q_1(X)*(1-H(t-1))$. The selected functions for $Q_1(X)$ have been listed in Table 2 in addition to their graphs which are plotted in Fig. 9. The average values of $Q_1(X)$ in all cases are the same or the selected profiles have the same static equivalent.

Fig. 10 shows that although the different profiles have the same static equivalent, they do not produce the same deflection. The parabolic and constant profiles lead to maximum and minimum displacements, respectively.

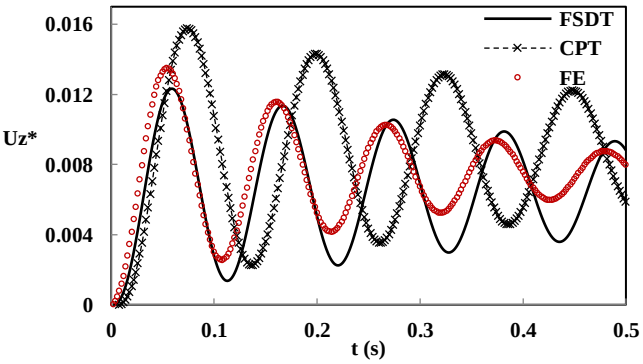

Figure 4. Transverse response near outer radius (r^*=0.933).

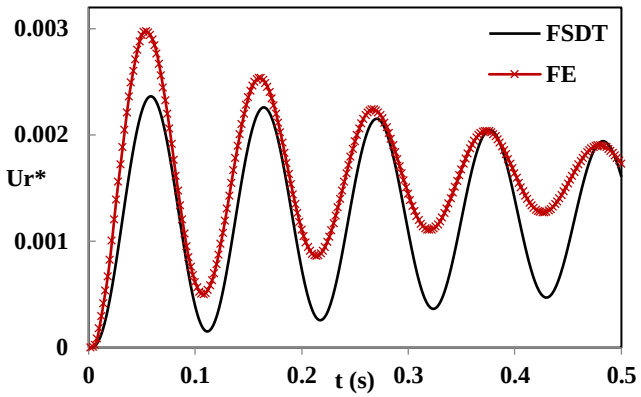

Figure 5. Radial response at r^*=0.767 and z=h/2.

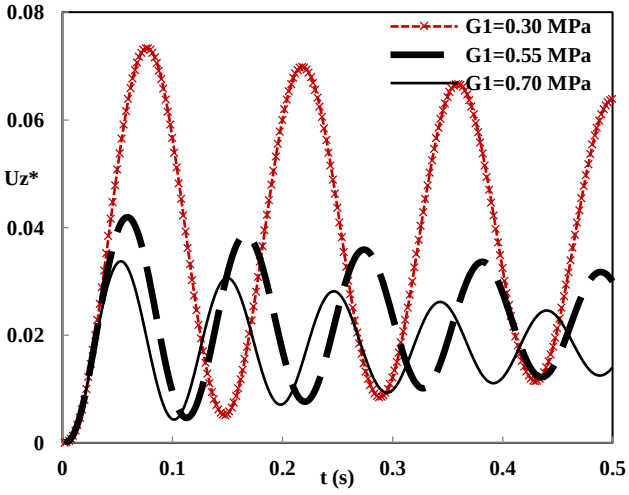

Figure 6. Effect of G_1 on the transverse response (FSDT).

The influence of viscosity on the transverse response has been shown in Fig. 7. By increasing the viscosity coefficient, the amplitude of transverse deflection decreases as expected, but the mean deflection has no significant change. The transverse response of an elastic plate can be obtained by setting $\tau \to 0$ in Eqs. (9b and 11). Fig. 8 shows the oscillations of the FSDT plate at $r=(r_i+r_o)/2$. It is observed that the vibrations are around the static deflection and as the load is removed, it oscillates around the zero point or it has free vibrations.

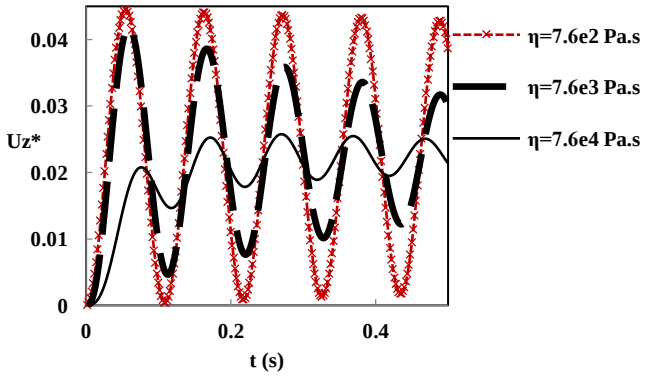

Figure 7. Effect of viscosity coefficient on transverse response at $r=(r_i+r_o)/2$ (FSDT).

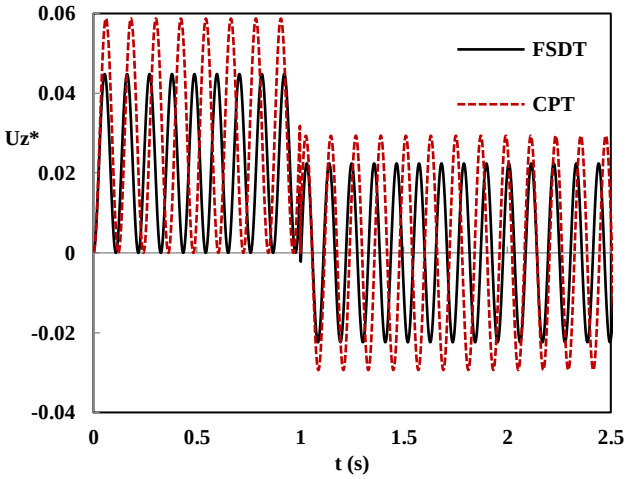

Figure 8. Transverse response of elastic plate by FSDT and CPT.

Table 2. Definition of different load profiles.

Load Function	$Q_1(X)$, q_0=5 N/m^2
Linear	(3X/7+8)/ q_0
Triangular	((2-0.8571.X)(1-H(-X-7))+(14+0.8571.X) *(H(-X-7)-H(-X-14)))/ q_0
Parabolic	(-9X²/98-9X/7+2)/ q_0
Sine	3.0551(1-sin(πX/14))/ q_0

6.4. Shear deformation

In the CPT, we have$u_{1=}$ - $\partial w_0/\partial r$ (in Eq. 1). These quantities have been reported in Table 3 at the location r^*=0.4 and time t=2 sec of a plate with characteristics that have been listed in Table 1. It is seen that the percentage difference between these quantities increases by decreasing the thickness in a viscoelastic plate or the effect of shear deformation is prominent for thick viscoelastic plates.

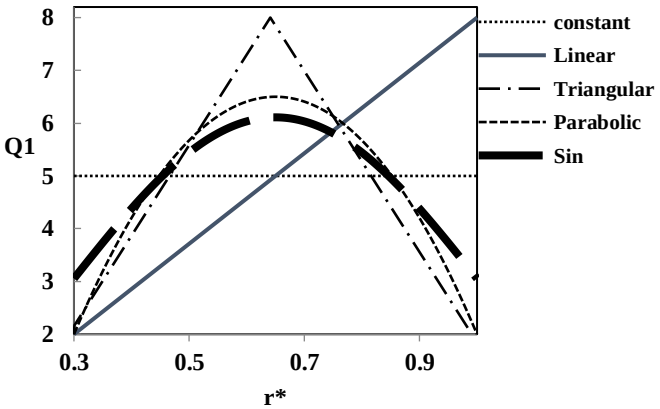

Figure 9. Different load profiles.

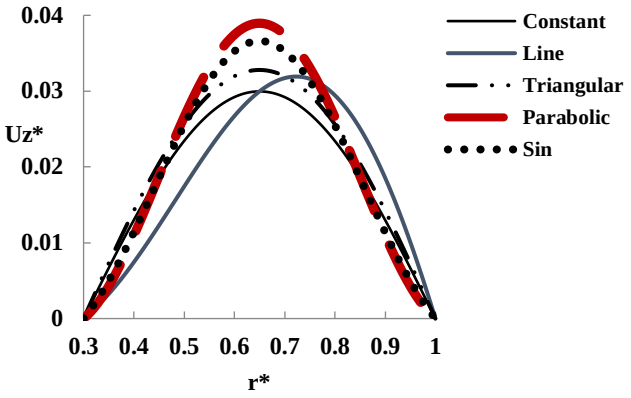

Figure 10. Transverse displacement for different load profiles (t=0.5 s).

Table 3. Effect of shear deformation (t=0.5s)

r_o/h	$-\partial w_0/\partial r$ (r^*=0.4)	u_1 (r^*=0.4)	Diff(%)
10	6.160e-4	5.700e-4	8.07
15	1.685e-3	1.620e-3	4.01
20	2.881e-3	2.810e-3	2.53
30	9.546e-3	9.410e-3	1.44
40	5.068e-2	5.042e-2	0.52

7. Conclusion

In this paper, an analytical procedure was presented for the response determination of viscoelastic annular plates under transverse excitation. The formulation was based on the FSDT and the results were compared with the CPT and FE. Some of the results are as the following:

- The introduced method is able to convert a system of partial differential equations with variable coefficients to systems of equations with constant coefficients.
- The present solution saves the time of computation considerably.
- The CPT has a time delay in response with respect to the FSDT and FE.
- The FSDT response is closer to the FE than the CPT (except at the beginning of applying load).
- The frequency of oscillation for the FSDT is in a good agreement with the FE rather than the CPT.
- The calculated amplitude of displacement using the FSDT is smaller than FE and CPT results.
- Increasing G_1not only decreases the average deflection but also increases the oscillation frequency which can be due to increasing the stiffness of the plate.
- By increasing the viscosity coefficient, the transverse deflection decreases as expected, but the mean deflection has no noticeable change.
- The parabolic and constant profiles result in the maximum and minimum displacements, respectively.
- The effect of shear deformation is significant in thick *viscoelastic* plates.

References

1. Zaremsky, G.J., *Aircraft brake*. 1993, Google Patents.
2. Chauhan, A. and Y. Kapoor, *Contact lens based bioactive agent delivery system*. 2011, Google Patents.
3. Ilyasov, M.H., *Dynamic stability of viscoelastic plates.* International journal of engineering science, 2007. **45**(1): p. 111-122.
4. Robertson, S.R., *Forced axisymmetric motion of circular, viscoelastic plates.* Journal of Sound and Vibration, 1971. **17**(3): p. 363-381.
5. Wang, Y.Z. and T.J. Tsai, *Static and dynamic analysis of a viscoelastic plate by the finite element method.* Applied Acoustics, 1988. **25**(2): p. 77-94.
6. Chen, T.M., *The hybrid Laplace transform/finite element method applied to the quasi-static and dynamic analysis of viscoelastic Timoshenko beams.* International Journal for Numerical Methods in Engineering, 1995. **38**(3): p. 509-522.
7. Abdoun, F., et al., *Forced harmonic response of viscoelastic structures by an asymptotic numerical method.* Computers & Structures, 2009. **87**(1-2): p. 91-100.
8. Assie, A.E., M.A. Eltaher, and F.F. Mahmoud, *The response of viscoelastic-frictionless bodies under normal impact.* International journal of mechanical sciences, 2010. **52**(3): p. 446-454.
9. Khalfi, B. and A. Ross, *Transient response of a plate with partial constrained viscoelastic layer damping.* International Journal of Mechanical Sciences, 2013. **68**: p. 304-312.
10. Amoushahi, H. and M. Azhari, *Static and instability analysis of moderately thick viscoelastic plates using a fully discretized nonlinear finite strip formulation.* Composites Part B: Engineering, 2014. **56**: p. 222-231.
11. Liang, X., et al., *Semi-analytical solution for three-dimensional transient response of functionally graded annular plate on a two parameter viscoelastic foundation.* Journal of Sound and Vibration, 2014. **333**(12): p. 2649-2663.
12. Gupta, A.K. and L. Kumar, *Vibration of non-homogeneous visco-elastic circular plate of linearly varying thickness in steady state temperature field.* Journal of Theoretical and Applied Mechanics, 2010. **48**(1): p. 255-266.
13. Pawlus, D., *Dynamic behaviour of three-layered annular plates with viscoelastic core under lateral loads.* Journal of Theoretical and Applied Mechanics, 2015. **53**(4): p. 775-788.
14. Panigrahi, S.K. and K. Das, *Ballistic impact analyses of triangular corrugated plates filled with foam core.* Advances in Computational Design, 2016. **1**(2): p. 139-154.
15. Kumar, A. and S. Panda, *Optimal damping in circular cylindrical sandwich shells with a three-layered viscoelastic composite core.* Journal of Vibration and Acoustics, 2017. **139**(6).
16. Behera, S. and P. Kumari, *Free vibration of Levy-type rectangular laminated plates using efficient zig-zag theory.* Advances in Computational Design, 2018. **3**(3): p. 213-232.
17. Ajri, M., M. Fakhrabadi, and A. Rastgoo, *Analytical solution for nonlinear dynamic behavior of viscoelastic nano-plates modeled by consistent couple stress theory.* Latin American Journal of Solids and Structures, 2018. **15**(9).
18. Ajri, M., A. Rastgoo, and M. Fakhrabadi, *Primary and secondary resonance analyses of viscoelastic nanoplates based on strain gradient theory.* International Journal of Applied Mechanics, 2018. **10**(10): p. 1850109.
19. Ajri, M. and M. Fakhrabadi, *Nonlinear free vibration of viscoelastic nanoplates based on modified couple stress theory.* Journal of Computational Applied Mechanics, 2018. **49**(1): p. 44-53.
20. Ajri, M., A. Rastgoo, and M. Fakhrabadi, *How does flexoelectricity affect static bending and nonlinear dynamic response of nanoscale lipid bilayers?* Physica Scripta, 2019. **95**(2): p. 025001.
21. Ajri, M., A. Rastgoo, and M. Fakhrabadi, *Non-stationary vibration and super-harmonic resonances of nonlinear*

viscoelastic nano-resonators. Structural Engineering and Mechanics, 2019. **70**(5): p. 623-637.
22. Sadd, M.H., *Elasticity: Theory, Applications, and Numerics*. 2009: Academic Press.
23. Wang, C.M., J.N. Reddy, and K.H. Lee, *Shear Deformable Beams and Plates: Relationships with Classical Solutions*. 2000: Elsevier.
24. Riande, E., et al., *Polymer Viscoelasticity: Stress and Strain in Practice*. 1999: CRC Press.
25. Suzuki, K., et al., *Axisymmetric vibrations of a vessel with variable thickness.* Bulletin of JSME, 1982. **25**(208): p. 1591-1600.
26. Nayfeh, A.H., *Introduction to Perturbation Techniques*. 2011: John Wiley & Sons.
27. Moshir, S.K., H.R. Eipakchi, and F. Sohani, *Free vibration behavior of viscoelastic annular plates using first order shear deformation theory.* Struct. Eng. Mech, 2017. **62**(5): p. 607-618.
28. Hagedorn, P. and A. DasGupta, *Vibrations and Waves in Continuous Mechanical Systems*. 2007: Wiley Online Library.
29. ANSYS Element Reference, www.ansys.stuba.sk

Appendix A.

For general boundary conditions, we substitute Eqs. (15a,b) into Eqs. (13b). It is yielded:

$$\sum_{m=1}^{\infty} L_{12}[A_{1m}(T_0,T_1)\phi_{2m}(X), A_{2m}(T_0,T_1)\phi_{3m}(X)] = 0;$$
$$\rightarrow \sum_{m=1}^{\infty} B_{12m} = 0 \ \ where:$$
$$B_{12m} = h^{*2}(g_{35}[A_{1m}(T_0,T_1), a_0, a_1]\phi''_{2m} \quad \text{(A1)}$$
$$-e\, g_{35}[\ddot{A}_{1m}(T_0,T_1), \beta G_1^*, G_0^*]\phi_{2m})$$
$$-12K_s(g_{35}[A_{2m}(T_0,T_1), \beta, 1]\phi'_{3m}$$
$$+g_{35}[A_{1m}(T_0,T_1), \beta, 1]\phi_{2m})$$

$$\sum_{m=1}^{\infty} L_{13}[A_{1m}(T_0,T_1)\phi_{2m}(X), A_{2m}(T_0,T_1)\phi_{3m}(X)] =$$
$$-g_{35}[Q^*, \beta G_1^*, G_0] \rightarrow \sum_{m=1}^{\infty} B_{13m} = -g_{35}[Q^*, \beta G_1^*, G_0];$$
$$where: ()' = \frac{d}{dX}; ()'' = \frac{d^2}{dX^2}; \ddot{()} = \frac{\partial^2}{\partial T_0^2} \quad \text{(A2)}$$
$$B_{13m} = h^*(K_s g_{35}[A_{2m}(T_0,T_1), 1, 1]\phi''_{3m}$$
$$-eg_{35}[\ddot{A}_{2m}(T_0,T_1), \beta G_1^*, G_0^*]\phi_{3m}$$
$$+K_s g_{35}[A_{1m}(T_0,T_1), \beta, 1]\phi'_{2m})$$

With the inner product of Eq. (A1) in φ_{2n} and Eq. (A2) in φ_{3n} we have:

$$h^{*2}(g_{35}[A_{1m}(T_0,T_1), a_0, a_1](\phi''_{2m}, \phi_{2m})$$
$$-e\, g_{35}[\ddot{A}_{1m}(T_0,T_1), \beta G_1^*, G_0^*](\phi_{2m}, \phi_{2m})) \quad \text{(A3)}$$
$$-12K_s(g_{35}[A_{2m}(T_0,T_1), \beta, 1](\phi'_{3m}, \phi_{2m})$$
$$+g_{35}[A_{1m}(T_0,T_1), \beta, 1](\phi_{2m}, \phi_{2m})) = 0$$
$$h^*(K_s g_{35}[A_{2m}(T_0,T_1), 1, 1](\phi''_{3m}, \phi_{3m})$$
$$-eg_{35}[\ddot{A}_{2m}(T_0,T_1), \beta G_1^*, G_0^*](\phi_{3m}, \phi_{3m}) \quad \text{(A4)}$$
$$+K_s g_{35}[A_{1m}(T_0,T_1), \beta, 1](\phi'_{2m}, \phi_{3m}))$$
$$= (-g_{35}[Q^*, \beta G_1^*, G_0], \phi_{3m})$$

Due to the orthogonality of the mode shapes, the non-zero solution can be found just for $m=n$. The inner product is defined as follows.

$$(p(X), q(X)) = \int_{X_i}^{X_o} p(X).q(X).dX \quad \text{(A5)}$$

Eqs. (A3,A4) are two coupled ordinary linear differential equations with constant coefficients. The same procedure can be applied for equations order-one. The obtained ordinary differential equations may be solved by the method explained in the text.